A coupled approach to model the effect of wear on the dynamics of bladed disks

26th INTERNATIONAL CONGRESS ON SOUND AND VIBRATION
7-11 July 2019, Montreal

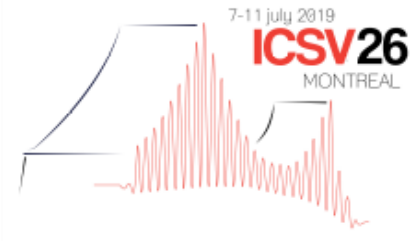

A COUPLED APPROACH TO MODEL THE EFFECT OF WEAR ON THE DYNAMICS OF BLADED DISKS

Lakshminarayana Reddy Tamatam, Daniele Botto *and* Stefano Zucca
Department of Mechanical and Aerospace Engineering
Politecnico di Torino, 10129 Torino, Italy
e-mail: lakshminarayana.tamatam@polito.it

This study proposes a technique to predict the effect of wear on the dynamics of structures with contact interfaces and the evolution of contact interface using a coupled static and dynamic multi-harmonic balance (MHBM) method. A multiscale approach is implemented, namely slow-scale for wear phenomena and fast-scale for the non-linear dynamic response. The wear is computed using wear energy approach and adaptive wear logic. The technique is applied to a tuned shrouded bladed disk on a single sector using cyclic symmetry property to predict the evolution of wear at the shroud contact interface and the corresponding change in dynamic response.
Keywords: non-linear structural dynamics, wear, contact interface, harmonic balance method

1. Introduction

A typical turbo-engine has assemblies made of thousands of contacts. The turbine blades experience high static and dynamic loads due to centrifugal forces, thermal strains and the fluctuating gas forces. These result in high vibration amplitudes which can lead to high cycle fatigue. Contact interfaces such as blade roots or tip shrouds are added to reduce the peak vibration amplitudes and provide friction damping. These interfaces are significant sources of non-linearity in the structural response of bladed disks. Friction damping affects the dynamics of structures with contacts introducing localized nonlinearity. The resulting partial or full tangential slip occurring at those interfaces leads to the hysteresis at the contact with energy dissipation and thereby causing wear [1]. The wear deteriorates the contact conditions over time and leads to the change in the dynamic response of the system. The current non-linear structural dynamic solvers are capable of predicting the dynamic response and the damping for the contact surfaces with a pristine surface. In reality, when the components are in service, wear could dramatically change the interface and the effects and could even lead to adverse impacts resulting in degraded performance and sometimes catastrophic failure. The surface changes at the microscopic level lead to the changes in dynamic response at the global level. The effect of these changes can be studied using FRFs (frequency response functions) for various loading conditions. Thus, to predict the effect of wear on the system dynamics, accurate wear modelling must be embedded in numerical solvers used to compute the nonlinear forced response. Armand et. al. has proposed a multiscale approach to predict the effect of fretting wear on the dynamic response of under platform dampers [2]. Loïc et. al. has proposed DLFT and HBM techniques to compute the effect of wear on the dynamics ([3], [4]).

The current research aims at developing and implementing a technique of predicting the effect of wear on the dynamics of structures with contact interfaces and also the evolution of contact interface using a proven static and dynamic coupled approach using multi-harmonic balance (MHBM) method [5]. With respect to the previous works existing in the literature ([6], [7]), the current approach allows the automatic update of the static pre-load distribution over the contact area during the non-linear dynamic analysis, without any need for a separate static analysis. The wear is computed using wear energy approach and adaptive wear logic. The technique is applied to a tuned shrouded bladed disk with cyclic symmetry properties to predict the effect of wear on the non-linear dynamic response and to visualize the evolution of the contact surface.

2. Methodology

The state-of-the-art method to compute the nonlinear response of structures with interfaces is the Harmonic Balance Method (HBM). This method assumes a periodic response under periodic excitation. The current study uses a more recent formulation of the HBM, which allows performing a coupled static and dynamic analysis of the system ([6]). The current test case is a tuned turbine bladed disk with shroud interface contacts as shown in Figure 1. Since the bladed disks are cyclic in nature, one can exploit by reducing the full bladed disk model to a single fundamental sector, by applying the proper boundary conditions at the sector interfaces, in nonlinear dynamic analysis ([5]).

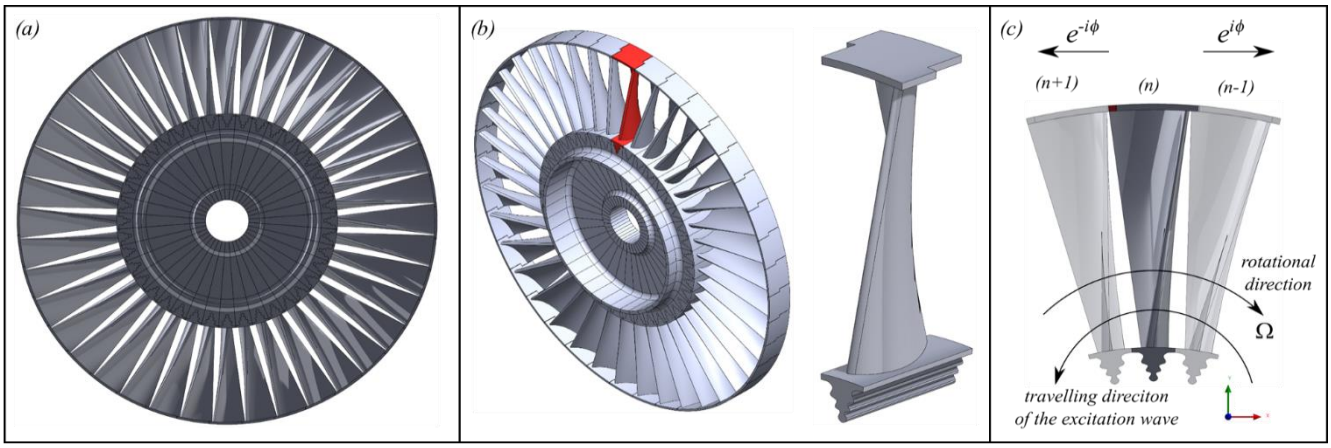

Figure 1: (a) Full bladed disk with shroud contact (b) A blade fundamental sector (c) Schematic view of cyclic symmetry for shrouded blade

2.1 Governing equations

The governing equation of motion of a tuned bladed disk with cyclic symmetry properties with contact interfaces can be written as:

$$\mathbf{m}\ddot{\mathbf{q}}_n(t) + \mathbf{c}\dot{\mathbf{q}}_n(t) + \mathbf{k}\mathbf{q}_n(t) = \mathbf{f}_n(t) + \mathbf{f}_{c,l}(\mathbf{q}_{n+1}, \mathbf{q}_n, \dot{\mathbf{q}}_{n+1}, \dot{\mathbf{q}}_n, t) + \mathbf{f}_{c,r}(\mathbf{q}_n, \mathbf{q}_{n-1}, \dot{\mathbf{q}}_{n-1}, \dot{\mathbf{q}}_n, t) \quad (1)$$

where $n = 1..N$ is a sector number; $\mathbf{m}$, $\mathbf{c}$ and $\mathbf{k}$ are the mass, viscous damping and stiffness matrices, $\mathbf{q}_n(t)$ is a displacement vector of n th sector; $\mathbf{f}_n(t)$ is the excitation force vector; $\mathbf{f}_{c,l}(\mathbf{q}_{n+1}, \mathbf{q}_n, \dot{\mathbf{q}}_{n+1}, \dot{\mathbf{q}}_n, t)$ and $\mathbf{f}_{c,r}(\mathbf{q}_n, \mathbf{q}_{n-1}, \dot{\mathbf{q}}_{n-1}, \dot{\mathbf{q}}_n, t)$ are nonlinear forces interaction vectors of nth sector and adjacent sectors from the left and from the right. They are dependent on displacements of nth sector in consideration and neighbouring $(n+1)$th and $(n-1)$th sectors.

To solve the equation (1) for periodic excitation using HBM, the periodic quantities are expressed as truncated series of harmonic terms:

$$\mathbf{q}(t) = \sum_{h=0}^{H} \hat{\mathbf{q}}^{(h)} e^{ih\omega t}\,;\; \mathbf{f}(t) = \sum_{h=0}^{H} \hat{\mathbf{f}}^{(h)} e^{ih\omega t}\,;\; \mathbf{f}_c(\mathbf{q}, \dot{\mathbf{q}}, t) = \sum_{h=0}^{H} \hat{\mathbf{f}}_c^{(h)}(\hat{\mathbf{q}}) e^{ih\omega t} \tag{2}$$

Time domain Equation (1) is turned to a nonlinear algebraic equation with complex coefficients:

$$\mathbf{D}^{(h)}\hat{\mathbf{q}}^{(h)} = \hat{\mathbf{f}}^{(h)} + \hat{\mathbf{f}}_c^{(h)}(\hat{\mathbf{q}})\ with\ h = 0..H \tag{3}$$

where $\mathbf{D}^{(h)} = \left(\mathbf{k}^{(h)} - h^2\omega^2\mathbf{m}^{(h)} + ih\omega\mathbf{c}^{(h)}\right)$, the equation (3) corresponds to the static $(h = 0)$ and dynamic $(h = 1..H)$ equations of the system respectively, coupled to each other by Fourier coefficients of the nonlinear contact force $\hat{\mathbf{f}}_c$ depending on the Fourier coefficients of the displacement $\hat{\mathbf{q}}$.

A travelling wave type excitation is considered. The inter-blade phase angle (IBPA) is defined as: $\emptyset = \frac{2\pi}{N}.EO$, where N is the number of blades, EO is the engine order. Due to the cyclic symmetry conditions, one can write the following coupling relationships for the displacements and forces on the left side with known right side:

$$\Delta\hat{\mathbf{q}}_{n,r}^{(h)} = \hat{\mathbf{q}}_{n,r}^{(h)} - \hat{\mathbf{q}}_{n-1,l}^{(h)};\ \Delta\hat{\mathbf{q}}_{n,r}^{(h)} = \hat{\mathbf{q}}_{n,r}^{(h)} - \hat{\mathbf{q}}_{n,l}^{(h)} e^{-ih\emptyset};\ \hat{\mathbf{f}}_{c,l}^{(h)} = -\hat{\mathbf{f}}_{c,r}^{(h)} e^{-ih\emptyset} \tag{4}$$

The residual equation is given by:

$$\mathbf{RES}^{(h)} = \mathbf{D}^{(h)}\hat{\mathbf{q}}^{(h)} - \hat{\mathbf{f}}^{(h)} - \hat{\mathbf{f}}_c^{(h)}(\hat{\mathbf{q}}) \tag{5}$$

The complex form residual equation is split into its real and imaginary components before solving as:

$$\mathbf{RES} = \left[\mathbf{RES}^{(0)}, \Re\left(\mathbf{RES}^{(1)}\right), \Im\left(\mathbf{RES}^{(1)}\right) \ldots \Re\left(\mathbf{RES}^{(H)}\right), \Im\left(\mathbf{RES}^{(H)}\right)\right]^{\mathrm{T}} \tag{6}$$

2.2 Contact Model

A contact model is needed to compute the nonlinear contact forces mentioned in the previous equations. A state-of-the-art node to node contact element, as shown in Figure 2, is used to model the contact. The solution of Equation (3) requires the contact forces $\mathbf{f}_c$ on the contact interface as input. The contact element is characterized by two linear springs in the tangential and normal direction with tangential (k_t) and normal (k_n) contact stiffness, at each node pair over the interface. The contact model allows to characterize and simulate three possible states – stick, slip and lift-off. At each element, the contact forces – tangential force $T(t)$ and the normal force $N(t)$ depend on the relative tangential and normal displacements of the corresponding node pair, namely $\mathbf{u}(t)$ and $\mathbf{v}(t)$ respectively. The friction limit value is defined by the Coulomb law as $\mu N(t)$, where μ is the coefficient of friction. Refer [6] for the working principle and application of the Jenkin's element contact model.

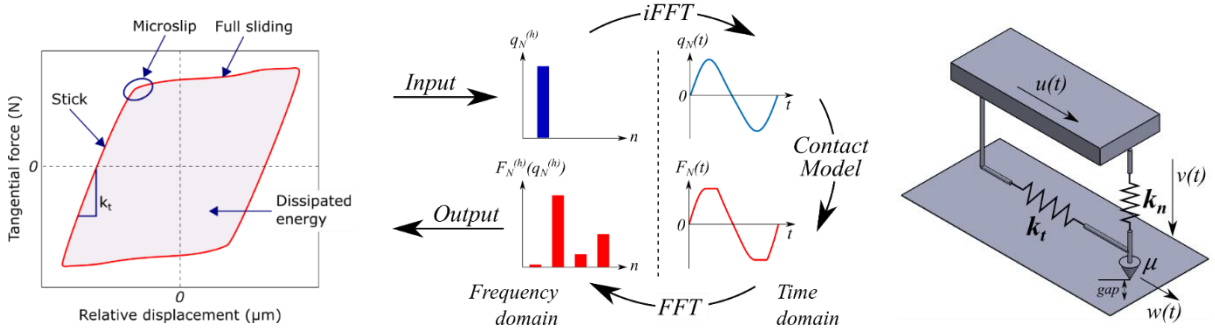

Figure 2: A typical hysteresis loop; Alternating Frequency Time (AFT) method to compute Fourier coefficients of contact forces; Jenkin's element contact model with variable normal load

The governing equation (3) is solved in the frequency domain using HBM, whereas the contact forces can only be computed in the time domain. Hence an Alternate Frequency/Time (AFT) method ([8]) is

employed. The relative displacements are converted from the frequency domain to time domain by applying IFFT and then passed through the contact model, and the contact forces are obtained in the time domain. FFT is then applied to convert to the Fourier coefficient of contact forces in the time domain as shown in [8]. Newton-Raphson logic is implemented for the iterative procedure. Since the Jacobian matrix needed to reduce the residual for Newton Raphson method is computationally intensive, an analytical Jacobian is implemented based on [9], [10]. The contact forces and the partial derivatives of the contact forces are computed and assembled in the Jacobian matrix. This greatly increases the speed of the solution. The contact forces and computation of the dynamic response is primarily based on the accurate input of contact stiffness. The closed-form solutions needed to compute the accurate tangential (k_t) and normal (k_n) contact stiffness to provide the contact model is provided in Ref [11], [12].

2.3 Wear computation

To model the evolution of wear on the contact interfaces, a wear energy approach is used ([13]) and the wear depth $\mathbf{v}_w$ associated at each node pair, worn out after Z_W cycles is computed as:

$$\mathbf{v}_w = \frac{Z_W}{A}\,\alpha E, \tag{7}$$

where A is the area associated with the node pair, α is the wear coefficient for a particular contact pair and E is the energy dissipated over one cycle. Since the nodal wear depth obtained at each vibration cycle is so small, there is no considerable change in the frequency response. Hence a wear acceleration technique is used. An adaptive wear logic is utilized by defining a parameter 'R'.

$$Z_W = \frac{R}{max(\Delta h_{ij})} \tag{8}$$

where, R is defined as maximum wear depth allowed at each wear iteration, either as a percentage of maximum static deflection, or as an acceptable error percentage in the permissible wear depth. Δh_{ij} is the maximum nodal wear depth at the contact patch at one vibration cycle. Δh_{ij} could vary from one vibration cycle to another, hence Z_W. The term $\mathbf{v}_w$ is then introduced to the 0th order coefficient of the relative displacement in the normal direction

$$\mathbf{v}(t) = \sum_{h=0}^{H} \hat{\mathbf{v}}^{(h)} e^{ih\omega t} - \mathbf{v}_w \tag{9}$$

and the HBM equation (3) can be solved, taking into account the effect of the wear depth on the static pre-load and on the nonlinear dynamics of the system simultaneously. Figure 3 gives an overview of the solution procedure starting from FE model up to computing the effect of wear on the dynamic response.

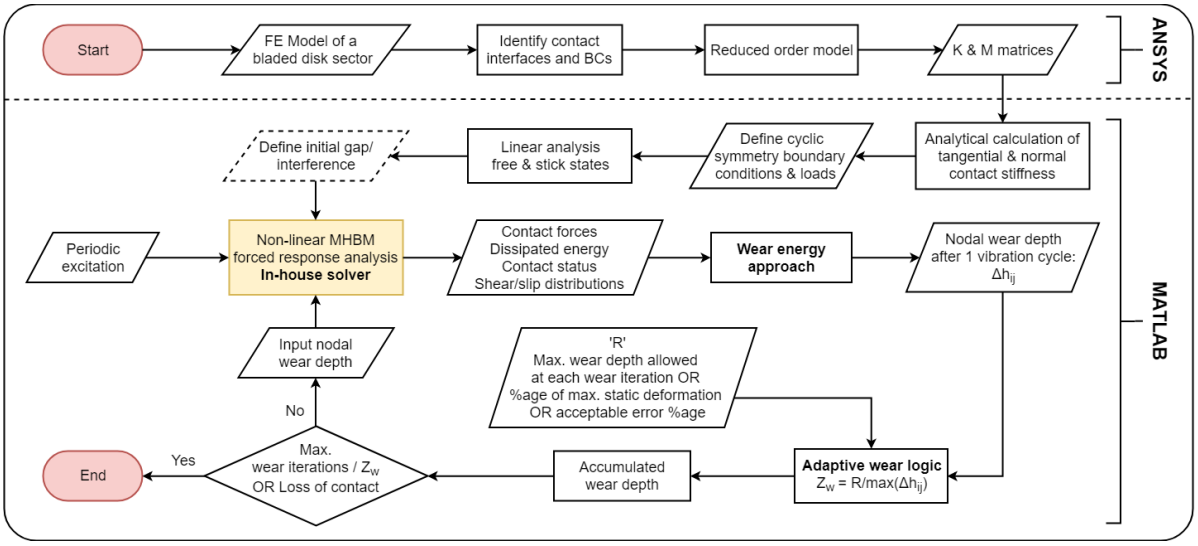

Figure 3: Solution algorithm flowchart to compute the non-linear dynamic response with wear

3. Test Case

A shrouded bladed disk consisting of 40 blades as shown in Figure 4(a) is used as a test case to demonstrate the impact of wear on shrouded bladed disks dynamics. The disk is assumed to be infinitely rigid and so fixed boundary conditions are applied at the blade root. In this way, the cyclic symmetry only operates through the blade-to-blade coupling at the shrouds.

A static torque is applied to the blade by two static forces F_{static}, in order to simulate the twisting effect, actually due to the centrifugal force in rotating blades, which produces the static pre-load at the shrouds. A concentrated periodic excitation $F_{dynamic}$ is also applied at a mid-span node of the airfoil. Figure 4(b) highlights the shroud contact patch consisting of 20 contact elements each side with a 5x4 grid. Figure 4(c) shows the contact elements distribution between right contact patch with an adjacent blade left contact patch with cyclic symmetry boundary conditions. The friction coefficient is assumed to be 0.5 and wear energy coefficient α as $2e3\ \mu m^3/J$. The analysis is performed by retaining the 0^{th} and the 1^{st} harmonics in equation (3). Using analytical methods to compute contact stiffness described in the previous section, k_t and k_n is computed to be 93 $N/\mu m$ and 113 $N/\mu m$ respectively.

In order to define the adaptive wear parameter R, the following logic is applied. The static deflection of the cantilever blade is computed under the action of the static forces. Then the average normal displacement of each contact surface is obtained. This value has been set as the maximum possible wear on each surface $\mathbf{v}_{w,max}$, since when such a depth is worn out the blades would vibrate freely without any contact with the adjacent blades. Finally, R is varied from 0.5% to 10% of $\mathbf{v}_{w,max}$ in order to investigate its effect on the accuracy of the model in predicting the evolution of the system dynamics.

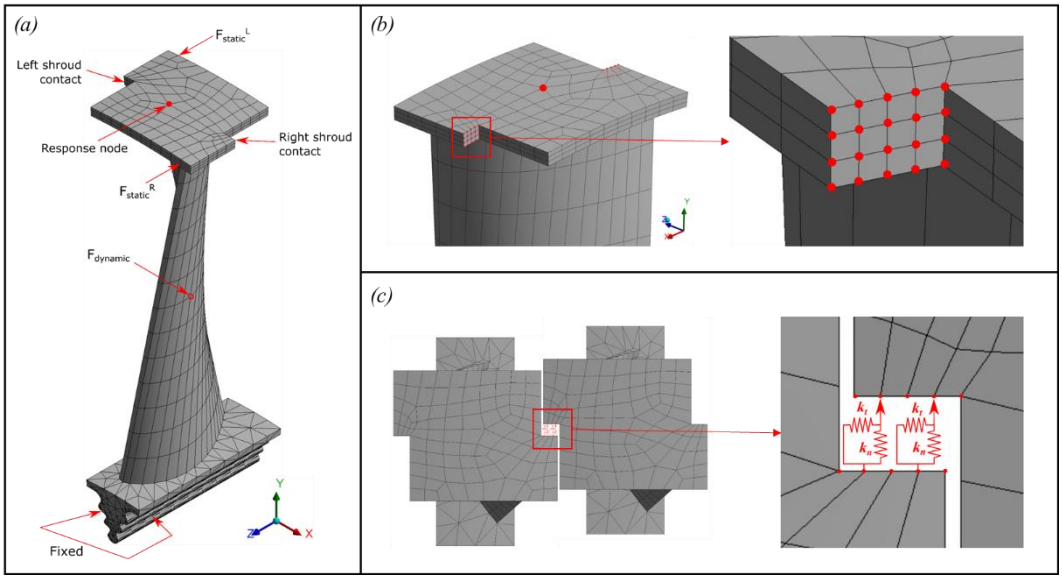

Figure 4: (a) FE model, boundary and loading conditions (b) Highlight of the shroud contact showing 20 contact nodes (c) Pictorial representation of the applied node-to-node contact model

Figure 5(a) shows the nodal diameter versus frequency map relationship up to 15 ND and Figure 5(b) shows the X, Y and Z response displacements at the output node for 1 EO excitation with the given loading conditions. Figure 6(a) shows the behaviour of the FRF curves for the given excitation forces with fixed F_{static} = 70 kN. The figure also includes a reference linear free state and stick state for comparison. With the increasing excitation force, the response frequency moves towards the free state frequency with varying maximum amplitudes. The linear free and stick peaks are shows for reference. Figure 6(b) shows the response for various engine order excitations along with the linear free state and stick state curves with the loading of F_{static} = 70 kN and $F_{dynamic}$ = 5 kN.

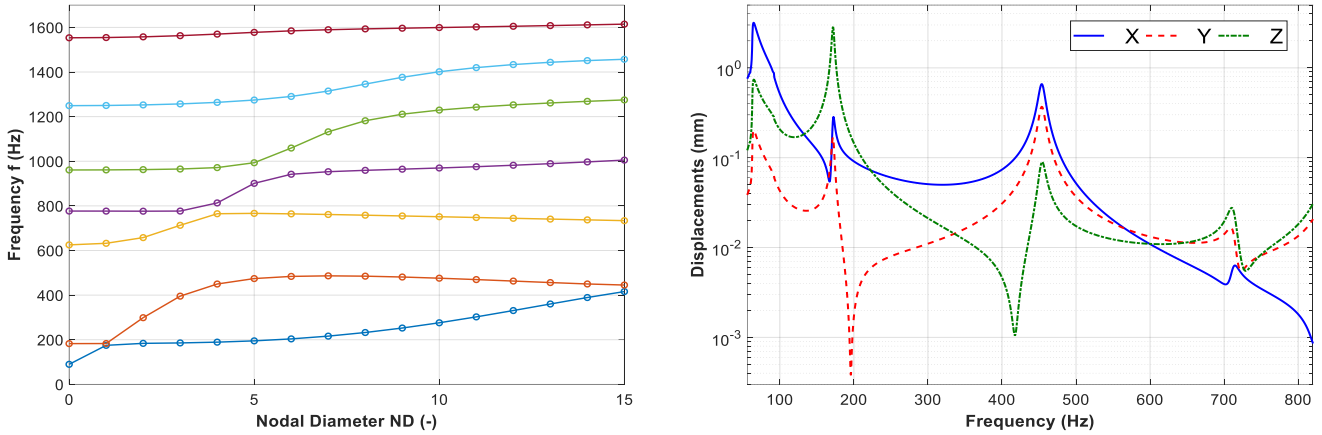

Figure 5: Nodal diameter map of shrouded blade (left), response of X, Y and Z axis for 1 EO excitation [F_{static} = 70 kN, $F_{dynamic}$ = 5 kN] (right)

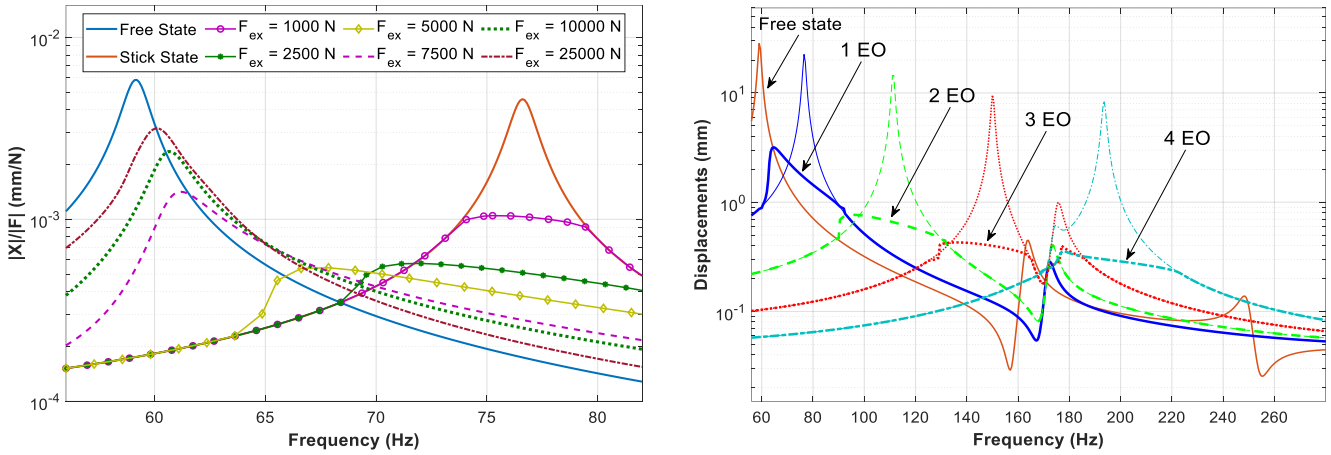

Figure 6: FRF for various excitation loads with fixed static load (left),
Response to various EO excitations with reference linear free and stick state peaks (right)

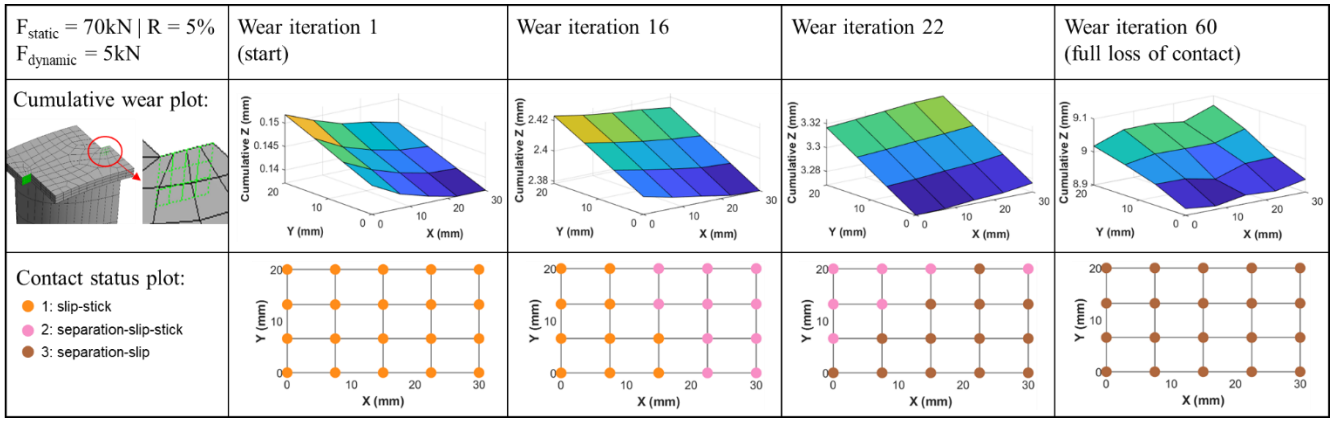

Figure 7: Tabular representation of the cumulative wear plot and contact status plot of the right shroud contact at different wear iterations until the loss of contact for given loading conditions

Figure 7 represents the cumulative wear plot and the contact status plot at various wear iteration intervals. For the mentioned loading conditions, the cumulative wear at the right shroud contact interface, the spatial wear distribution and also the contact status at each node can be visualized. At the beginning of the wear stage, the contact is in slip-stick state with uniform pressure distribution. As wear progresses, some of the contact nodes are in separation-slip-stick and eventually separation-slip before the complete loss of contact. For simplicity only one loading condition is shown. The same procedure can be used to

visualize various loading conditions and the adaptive logic parameter R with an accurate insight at the interface. Figure 8(a) shows the response with the impact of wear and how the response changes with the progress in wear. Figure 8(b) shows the number of wear cycles Z_W at each wear iteration as wear progresses up to the loss of contact. It is worthy to mention that the curve shown in this figure is not unique but it depends on the loading conditions and the pressure distribution at the contact.

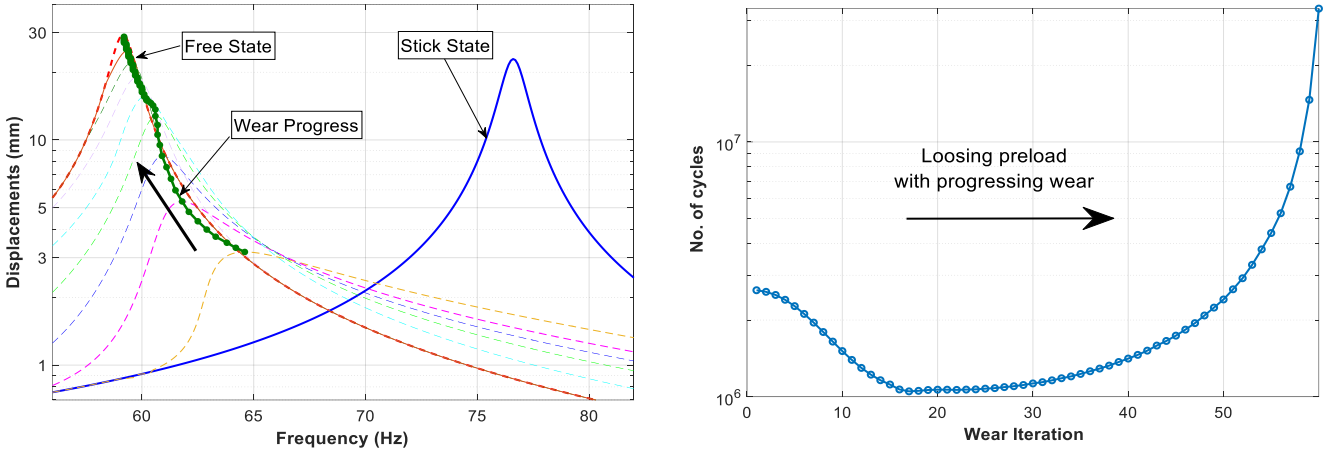

Figure 8: Impact of wear on the response with reference free and stick peaks (left), Impact of wear on the number of cycles at each wear iteration until full loss of contact [F_{static} = 70 kN, $F_{dynamic}$ = 5 kN, R = 5%]

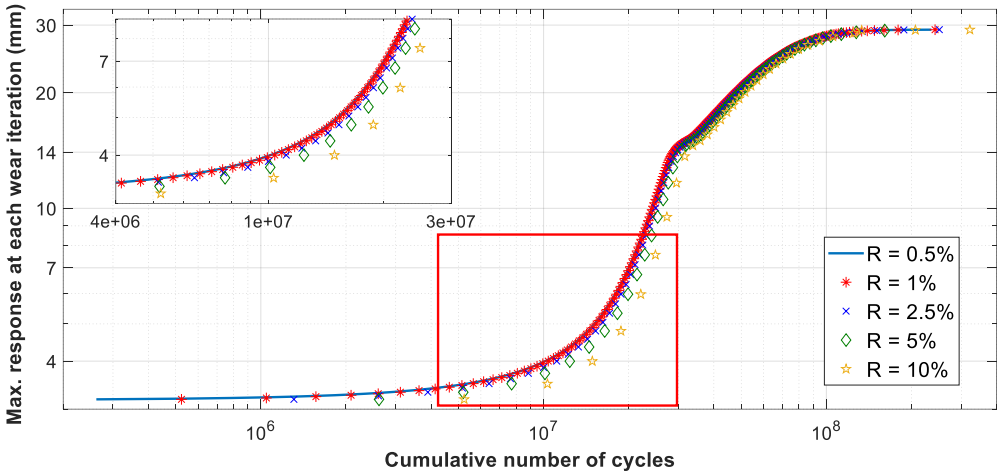

Figure 9: Maximum response at each wear iteration vs the cumulative number of cycles for different values of R

It is benifical to track the maximum response with respect to the cumulative number of cycles as it provides the stage at which the ampltidue increases considerably. Figure 9 shows the maximum response versus cumulative number of cycles until full loss of contact. Results show that for higher values of R, the rate of change of the response is under-estimated, leading to non-conservative predictions.

Table 1: Comparison of impact of wear analysis with non-linear dynamic response solver for different values of R [F_{static} = 70 kN, $F_{dynamic}$ = 5 kN]

R	Computational time	Total no. of wear iterations	Max. total wear depth (mm)	Error in wear depth (%)
0.5 %	5 hr 10 min	599	9.04	-
1 %	3 hr 4 min	301	9.05	0.11
2.5 %	1 hr 16 min	123	9.06	0.22
5 %	36 min	61	9.07	0.33
10 %	19 min	35	9.31	2.99

Table 1 summarizes the impact of wear analysis on the non-linear dynamic response for the given loading conditions. Smaller values of R, on one side, imply a higher number of wear iterations and longer computational times, but, on the other side, they enable to accurately track interface behaviour and predict the onset of full loss of contact. The choice of R depends on the tradeoff between accuracy and time.

4. Conclusions

The current work proposes a technique of implementing wear on the shroud contact elements of a tuned bladed disk with cyclic symmetry properties and to study the effect of wear on the dynamics using a coupled static-dynamic HBM formulation. Thanks to the proposed method, the effect of wear on the static pre-load distribution over the contacts is automatically taken into account during the nonlinear analysis, allowing to track the contact evolution and the changes in the dynamic behaviour of the system.

ACKNOWLEDGEMENTS

This project has received funding from the European Union's Horizon 2020 research and innovation programme under the Marie Sklodowska-Curie grant agreement No 721865.

REFERENCES

[1] R. B. Waterhouse, "Fretting wear," *Wear*, vol. 100, no. 1–3, pp. 107–118, 1984.

[2] J. Armand, L. Pesaresi, L. Salles, and C. W. Schwingshackl, "A Multiscale Approach for Nonlinear Dynamic Response Predictions with Fretting Wear," *J. Eng. Gas Turbines Power*, vol. 139, no. 2, pp. 1–7, 2017.

[3] L. Salles, A. M. Gouskov, L. Blanc, F. Thouverez, and P. Jean, "Dynamic analysis of fretting-wear in joint interface by a multiscale harmonic balance method coupled with explicit or implicit integration schemes," *ASME. Turbo Expo Power Land, Sea, Air, Vol. 6 Struct. Dyn. Parts A B*, vol. 6, pp. 1003–1013, 2010.

[4] L. Salles, L. Blanc, A. Gouskov, P. Jean, and F. Thouverez, "Dual Time Stepping Algorithms With the High Order Harmonic Balance Method for Contact Interfaces With Fretting-Wear," *J. Eng. Gas Turbines Power*, vol. 134, no. 4, p. 032503, 2011.

[5] L. R. Tamatam, D. Botto, and S. Zucca, "Effect of wear on the dynamics of structures with contact interfaces by a coupled static / dynamic multi-harmonic balance method Acknowledgments," in *First International Nonlinear Dynamics Conference. Book of abstracts*, 2019, no. 1, pp. 129–130.

[6] C. M. Firrone, S. Zucca, and M. M. Gola, "The effect of underplatform dampers on the forced response of bladed disks by a coupled static/dynamic harmonic balance method," *Int. J. Non. Linear. Mech.*, vol. 46, no. 2, pp. 363–375, 2011.

[7] S. Zucca and C. M. Firrone, "Nonlinear dynamics of mechanical systems with friction contacts: Coupled static and dynamic Multi-Harmonic Balance Method and multiple solutions," *J. Sound Vib.*, vol. 333, no. 3, pp. 916–926, 2014.

[8] T. M. Cameron and J. H. Griffin, "An Alternating Frequency / Time Domain Method for Calculating the Steady-State Response of Nonlinear Dynamic Systems," *J. Appl. Mech.*, vol. 56, p. 149, 1989.

[9] C. Siewert, L. Panning, J. Wallaschek, and C. Richter, "Multiharmonic Forced Response Analysis of a Turbine Blading Coupled by Nonlinear Contact Forces," *J. Eng. Gas Turbines Power*, vol. 132, no. 8, p. 082501, 2010.

[10] A. Cardona, A. Lerusse, and M. Géradin, "Fast Fourier nonlinear vibration analysis," *Comput. Mech.*, vol. 22, no. 2, pp. 128–142, 1998.

[11] M. Allara, "A model for the characterization of friction contacts in turbine blades," *J. Sound Vib.*, vol. 320, no. 3, pp. 527–544, 2009.

[12] M. Ciavarella, D. A. Hills, and G. Monno, "The influence of rounded edges on indentation by a flat punch," *Proc. Inst. Mech. Eng. Part C J. Mech. Eng. Sci.*, vol. 212, no. 4, pp. 319–327, 1998.

[13] M. Z. Huq and J. P. Celis, "Expressing wear rate in sliding contacts based on dissipated energy," *Wear*, 2002.